Title

CaMKIIδ post-translational modifications increase affinity for calmodulin inside cardiac ventricular myocytes

Authors

Simon, Mitchell

Ko, Christopher Y

Rebbeck, Robyn T

et al.

Publication Date

2021-12-01

DOI

10.1016/j.yjmcc.2021.08.002

HHS Public Access

Author manuscript

J Mol Cell Cardiol. Author manuscript; available in PMC 2021 December 29.

Published in final edited form as:

J Mol Cell Cardiol. 2021 December ; 161: 53–61. doi:10.1016/j.yjmcc.2021.08.002.

CaMKIIδ post-translational modifications increase affinity for calmodulin inside cardiac ventricular myocytes

Mitchell Simon[a,1], **Christopher Y. Ko**[a,1], **Robyn T. Rebbeck**[b], **Sonya Baidar**[a], **Razvan L. Cornea**[b], **Donald M. Bers**[a,*]

[a]Department of Pharmacology, University of California, Davis, CA, USA

[b]Department of Biochemistry, Molecular Biology, and Biophysics, University of Minnesota, Minneapolis, MN, USA

Abstract

Persistent over-activation of CaMKII (Calcium/Calmodulin-dependent protein Kinase II) in the heart is implicated in arrhythmias, heart failure, pathological remodeling, and other cardiovascular diseases. Several post-translational modifications (PTMs)—including autophosphorylation, oxidation, *S*-nitrosylation, and *O*-GlcNA-cylation—have been shown to trap CaMKII in an autonomously active state. The molecular mechanisms by which these PTMs regulate calmodulin (CaM) binding to CaMKIIδ—the primary cardiac isoform—has not been well-studied particularly in its native myocyte environment.

Typically, CaMKII activates upon Ca-CaM binding during locally elevated $[Ca]_{free}$ and deactivates upon Ca-CaM dissociation when $[Ca]_{free}$ returns to basal levels. To assess the effects of CaMKIIδ PTMs on CaM binding, we developed a novel FRET (Forster resonance energy transfer) approach to directly measure CaM binding to and ¨ dissociation from CaMKIIδ in live cardiac myocytes. We demonstrate that autophosphorylation of CaMKIIδ increases affinity for CaM in its native environment and that this increase is dependent on $[Ca]_{free}$. This leads to a 3-fold slowing of CaM dissociation from CaMKIIδ (time constant slows from ~0.5 to 1.5 s) when $[Ca]_{free}$ is reduced with physiological kinetics. Moreover, oxidation further slows CaM dissociation from CaMKIIδ T287D (phosphomimetic) upon rapid $[Ca]_{free}$ chelation and increases FRET between CaM and CaMKIIδ T287A (phosphoresistant).

The CaM dissociation kinetics–measured here in myocytes–are similar to the interval between heartbeats, and integrative memory would be expected as a function of heart rate. Furthermore, the PTM-induced slowing of dissociation between beats would greatly promote persistent CaMKIIδ activity in the heart. Together, these findings suggest a significant role of PTM-induced changes in

*Corresponding author at: Department of Pharmacology, University of California, Davis, 451 Health Sciences Drive, Davis, CA 95616, USA. dmbers@ucdavis.edu (D.M. Bers).

[1]These two authors contributed equally to this work

Disclosures

None.

Declaration of Competing Interest

None.

Supplementary data to this article can be found online at https://doi.org/10.1016/j.yjmcc.2021.08.002.

CaMKIIδ affinity for CaM and memory under physiological and pathophysiological processes in the heart.

Keywords

CaMKII; Calmodulin; Post-translational modifications; Calcium; Cardiac myocyte

1. Introduction

CaMKII (Calcium/Calmodulin-dependent protein Kinase II) is a central regulator of Ca handling, electrophysiology, transcription, and other processes in the heart [1–6]. Its persistent over-activation is implicated in arrhythmias, heart failure, pathological remodeling, and other diseases [1,7,8]. Elucidating the molecular mechanisms of this persistent CaMKII activity will improve our understanding of its role in physiological and pathophysiological cardiac processes. Specifically, we aim to quantify how post-translational modifications (PTMs) of CaMKIIδ affect its affinity for calmodulin (CaM) in the heart.

Ca-CaM is the primary activator of CaMKII, but several PTMs in the CaMKII regulatory domain, including autophosphorylation, oxidation, *S*-nitrosylation, and O-GlcNAcylation can regulate the kinase. These PTMs may trap CaMKII in autonomously active conformations that increase CaMKII activity and may all contribute to cardiac dysfunction in disease states [9–11]. Schulman's group showed that autophosphorylation of CaMKIIα (neuronal isoform) increases its affinity for CaM by ~1000-fold in cell lysates [12], identifying a molecular mechanism for this increased activity. Whether this also occurs with CaMKIIδ, the primary cardiac isoform [13], has not been directly measured—especially in its native myocyte environment. Similarly, whether all of these PTMs affect CaMKII affinity for CaM is undetermined.

Typically, CaMKII activates upon Ca-CaM binding during elevated $[Ca]_{free}$ and deactivates upon Ca-CaM dissociation when $[Ca]_{free}$ returns to basal levels [14]. The aforementioned PTMs trap CaMKII in an autonomously activated state even after $[Ca]_i$ declines and CaM dissociates [9–11,15]. The increase in CaM affinity of autophosphorylated CaMKIIα contributes to this uncoupling of CaMKII activity from $[Ca]_{free}$ and increased activity implicated in memory and several diseases.

A hallmark of CaMKIIα regulation is its ability to phosphorylate itself on an adjacent subunit within homomultimers at T286 (or T287 in CaMKIIδ and other isoforms) [16]. This leads to autonomous activity, which reportedly ranges from 20 to 100% of fully activated CaMKII (the more recent reports settle towards the lower-middle end of this range) [17,18]. The increase in CaM affinity with autophosphorylation of CaMKIIα may not fully recapitulate in CaMKIIδ or be relevant to conditions in the heart. The 4 CaMKII isoforms have different CaM affinities and activation patterns, reflecting their unique roles in tissues throughout the body [19]. Determining how autophosphorylation of CaMKIIδ affects its CaM affinity is necessary for understanding the dynamic role of this mechanism in cardiac myocytes.

Furthermore, understanding how autophosphorylation affects CaM affinity may indicate the mechanism by which other PTMs—oxidation, *S*-nitrosylation, and *O*-GlcNAcylation—trap CaMKII in an autonomously activated state [9–11]. These PTMs implicate CaMKII in additional disease regimes and may interact to regulate the kinase additively or synergistically [20]. While specific amino acid sites for these PTMs have been identified, a detailed mechanism for their regulation of CaM-CaMKII affinity and dissociation kinetics has not. Quantifying how autophosphorylation affects CaM affinity creates a framework for understanding how other PTMs regulate CaMKIIδ under a broad range of conditions in the heart.

CaMKII is also regulated by the proteins that anchor it to its targets/ substrates [17,21]; therefore, measuring CaM affinity in CaMKIIδ's native myocyte environment will be especially physiologically relevant. Free cytosolic [CaM] is relatively low in cardiac myocytes (50–100 nM) [22] and CaMKII has relatively low Ca_4CaM affinity ($K_{0.5}$ ~30 nM) when compared to other CaM targets. Thus, very high local $[Ca]_i$ is required to raise $[Ca_4CaM]$ sufficiently to activate CaMKII. In the heart, two CaMKIIδ splice variants are expressed (δ_C and δ_B) which are identical other than an 11 amino acid nuclear localization sequence in δ_B. In ventricular cardiac myocytes, CaMKII is preferentially localized at the *Z*-lines where Ca flux from nearby L-type calcium and sarcoplasmic reticulum (SR) Ca release channels RyR2 [23–26] create the locally high $[Ca]_{free}$ (≥20 μM) and [Ca-CaM] sufficient for CaMKIIδ activation at each beat [27–29]. Quantifying PTM-induced changes in CaMKIIδ's affinity for CaM in its native environment will provide a more accurate understanding of this mechanism in the heart.

Lastly, capturing the kinetic consequences of PTM-induced changes in CaMKIIδ affinity for CaM is essential for determining whether they are relevant at physiological timescales. In cardiac myocytes, beat-to-beat changes in $[Ca]_{free}$ are mirrored by dynamic changes in Ca-CaM concentrations [30]. At higher pacing frequencies or heart rates Ca-CaM levels integrate [29] as does CaMKII activity (as predicted by computational simulations) [28]. Quantifying relative changes in CaM dissociation kinetics from CaMKIIδ will improve our understanding of the role of this mechanism in the dynamic cardiac environment.

In this study, we develop a novel intermolecular FRET approach to directly measure CaM binding to CaMKIIδ in live cardiac myocytes. We demonstrate that autophosphorylation of CaMKIIδ increases affinity for CaM in its native environment and that this increase is dependent on $[Ca]_{free}$. This leads to a 3-fold slowing of CaM dissociation from CaMKIIδ when $[Ca]_{free}$ is rapidly reduced. Furthermore, the interaction of autophosphorylation and oxidation leads to even slower CaM dissociation. Together these findings suggest a significant role of PTM-induced changes in CaMKIIδ affinity for CaM in physiological and pathophysiological processes that can promote chronic CaMKIIδ activity in the heart.

2. Methods

All animal procedures were in accordance with protocols approved by the Institutional Animal Care and Use Committee at the University of California, Davis (#19721) conforming to the Guide for the Care and Use of Laboratory Animals published by the

US National Institutes of Health (8th edition, 2011). The data used for this article will be shared upon request to the corresponding author.

2.1. Rabbit ventricular myocyte isolation and adenoviral transfection

Ventricular cardiac myocytes were isolated from male New Zealand White rabbits (3–4 months old, 2.5–3 kg) as previously described [31,32]. Briefly, the rabbits were injected with heparin (5000 U/kg body weight) before inducing general anesthesia with propofol (10 mg/kg body weight) followed by isoflurane inhalation (2–5% in 100% O_2) throughout the procedure. Absence of pain reflexes was used to verify deep surgical anesthesia prior to euthanasia via surgical excision of the heart.

The aorta was cannulated on a constant flow Langendorff system and retrograde perfused with nominally Ca^{2+}-free normal Tyrode's solution (37 °C; gassed with 100% O_2). Ventricular myocytes were digested using collagenase type II (Worthington Biochemical Corp.) and protease type XIV (Sigma-Aldrich).

Isolated myocytes were plated ~1.2×10^4 cells per well on laminin-coated 8-well chambers (ibidi, polymer #1.5) and cultured in PC-1 medium (Lonza) with purified adenovirus to transduce CaMKIIδ_C-GFP WT, T287A, or T287D (MOI: 100; 3.0×10^{10}, 7.4×10^8 6.6×10^8 particles/mL, respectively). GFP was fused to the association domain (C terminus) of the CaMKIIδ_C constructs (*R. norvegicus*) via a 20-residue linker. Cells were cultured for 24–48H at 37 °C to allow sufficient CaMKIIδ expression for imaging, which in our lab results in ~60% expression over the endogenous CaMKIIδ [27]. After culture, myocytes were transferred to a normal Tyrode's buffer (NT, nominally Ca^{2+}-free) with studies performed at room temperature (22–23 °C) at pH 7.2.

2.2. Internal solutions and CaM loading

To begin experiments prior to sarcolemmal permeabilization, NT was replaced by an internal solution containing 0.5 mM 5,5' DiBromo BAPTA tetrapotassium salt, 120 mM aspartic acid potassium salt, 0.5 mM $MgCl_2$, 10 mM HEPES, and 8% dextran. Ventricular myocytes were then permeabilized in nominally Ca^{2+}-free (0 Ca) internal solution with saponin (20 μg/mL) for 1–3 min and washed in nominally 0 Ca internal solution for >3 min. MaxChelator [33] was used to calculate $CaCl_2$ concentrations necessary for a range of $[Ca]_{free}$ solutions from <20 nM to 20 μM. $[Ca]_{free}$ in solutions was verified with Fura-2 fluorescence ratio measurements (Supplemental Fig. S1). For most experiments, $[Ca]_{free}$ needed to be much higher than 500 nM to achieve substantial CaM binding to CaMKII, but steady-state elevations of $[Ca]_{free}$ to the required 2–20 μM range produce massive hypercontracture even in the presence of 20–80 nM cytochalasin D. To prevent this hypercontracture, ATP and its precursors were omitted from the internal solution to induce an ATP-depleted rigor state of the myofilaments and stabilization of myocyte ultrastructure. Since ATP is a physiological Ca^{2+} and Mg^{2+} buffer, changes in $[Ca^{2+}]_{free}$ and $[Mg^{2+}]_{free}$ resulting from the omission of ATP in the buffered solutions above were calculated using MaxChelator and compensated appropriately.

CaM was labeled with Alexa Fluor 568 (AF568; as FRET acceptor) at a single Cys substituted at position T26 (F-CaM), as previously described [34]. F-CaM (typically 100

nM) was added to the internal solution in permeabilized cells for >60 min unless noted otherwise.

For rapid Ca chelation experiments, internal solution with 36 mM BAPTA was added to the bath for a final concentration of 20 mM. BAPTA (and Br_2-BAPTA) are advantageous over EGTA because of rapidity of Ca chelation and limited pH perturbation. The pipette was positioned directly above the objective lens and surface of the bath, and a syringe pump (Genie Touch, Kent Scientific Corporation) was used for consistent, local delivery of the BAPTA internal solution.

2.3. Imaging

A Nikon Eclipse T*i* confocal (40× objective) was used for AF568 (acceptor) photobleach in F-CaM association and dissociation experiments. Solid state laser illumination at 488 nm was used for donor GFP excitation and 561 nm was used to directly excite AF568 (of F-CaM). Virtual filter settings were used to collect GFP donor emissions at 495–550 nm (FWHM) and F-CaM acceptor emissions at 600–680 nm (FWHM). For acceptor photobleach experiments, circular regions of interest (ROI; ~10 μm) were selected for intense exposure to 561 nm laser to bleach F-CaM down to ~10% of the pre-bleach fluorescence intensity.

A Zeiss LSM 5 Live confocal (40× objective) was used for rapid BAPTA delivery experiments. A 488 nm solid state laser was used for GFP (FRET donor) excitation, and emission was recorded at 500–525 nm (FWHM). AF568 (acceptor) emission was recorded at >550 nm.

Fluorescence lifetime imaging experiments (FLIM) experiments were performed on a Leica Falcon confocal (SP8; 40× objective). A white-light femtosecond frequency-pulsed laser excited the donor at 488 nm. Donor emissions were acquired at 490–550 nm, as were arrival times for time correlated single photon counting (TCSPC). Additional background, context, and rationale for FRET and FLIM-FRET methods used in this study are provided in Supplementary Methods.

2.4. Analysis

Cells from fluorescence intensity images were analyzed using ImageJ [35]. Curve fitting for rapid CaM dissociation experiments was performed with custom code written in Python using NumPy, SciPy, and Matplotlib packages [36–38].

Leica Application Suite X software was used to analyze FLIM-FRET cell images. Curves were fit to TCSPC decay histograms to determine donor fluorescence lifetime (FLT). A bi-exponential fit was used to account for autofluorescence [39]. All cells had a minimum mean of 1000 photons recorded per pixel to allow precise curve fitting [40].

Statistical analyses were performed at the level of the myocyte (n), which served as the vehicle within which the molecular-level interactions of interest for this study between CaMKII and CaM were evaluated. Data are presented as mean with 95% confidence interval. Normality and equality of group variance were assessed with the Kolmogorov-

Smirnov and Brown-Forsythe tests, respectively. One-way ANOVA followed by the post-hoc multiple comparison test implemented is noted in figure legends. GraphPad Prism 8.0 was used for data analysis. Differences were considered statistically significant if $P < 0.05$. P-values are noted in figures/figure legends.

3. Results

Fig. 1 illustrates that FRET between CaMKIIδ_C-GFP (donor) and F-CaM (acceptor) is a dynamic sensor for binding between the two proteins in rabbit ventricular myocytes. This allows the quantification of changes in CaMKIIδ affinity for CaM in its native environment. The permeabilized myocyte allows precise control over $[Ca]_{free}$ and [F-CaM] enabling quantitative analysis. At 500 nM $[Ca]_i$, F-CaM shows high co-localization at the *Z*-line where CaMKIIδ_C-GFP coexists (Fig. 1A, right). However, this F-CaM is likely to reflect F-CaM largely bound to RyR2 along the Z-line, that occurs at high affinity (K_d ~20 nM at 50 nM $[Ca]_i$ [41] and much higher affinity at 500 nM $[Ca]_i$ [22]). Indeed, at 500 nM $[Ca]_i$, where CaM sites on RyR2 should be fully saturated, bright striations are clear in the directly excited F-CaM signal (F_{AA}) in Fig. 1A–B (top). This does not complicate our measurements of F-CaM-CaMKIIδ_C-GFP, because when F-CaM was almost completely photobleached, there was nearly undetectable enhancement of donor CaMKIIδ_C-GFP fluorescence (mean of 0.047 ± 0.034 SD, green point). This indicates insignificant FRET between F-CaM-RyR2 and CaMKIIδ_C-GFP compared to that expected if significant F-CaM binding to CaMKIIδ_C-GFP had occurred at this $[Ca]_{free}$. However, raising $[Ca]_{free}$ to 1 μM (which does not further increase CaM-RyR binding) resulted in clearly detectable FRET between F-CaM and CaMKIIδ_C-GFP, as evidenced by 21.2 ± 5.8% increase in GFP fluorescence upon photobleached ROI, indicative of significant F-CaM binding to CaMKIIδ_C-GFP (Fig. 1A, lower panel red point in Fig. 1B; see also movie in Supplemental Fig. S2). This F-CaM binding, which becomes significant at 1 μM $[Ca]_{free}$, is consistent with reports that CaMKII is a relatively low-affinity CaM target in cells [28,29]. Indeed, the affinity for Ca_4CaM binding to CaMKIIδ (K_d = 34 nM [19]) is dramatically lower than for calcineurin (K_d = 0.028 nM [42]). This has major implications to where and when these two Ca-CaM targets are activated by dynamic cytosolic $[Ca]_{free}$ transients [14].

Notably, this degree of FRET was obtained with 100 nM F-CaM and 1 μM $[Ca]_{free}$ which represent the upper-end of the global physiological $[CaM]_{free}$ and $[Ca]_{free}$ in cardiac myocytes [22]. Thus, these acceptor photobleach experiments demonstrate that FRET is a robust reporter of F-CaM binding to CaMKIIδ_C-GFP in its native environment with physiologically consistent behavior.

Destructive acceptor photobleach experiments are not practical for kinetic measurements or quantifying changes in CaMKIIδ affinity for CaM. Therefore, obtaining changes in FRET by promoting F-CaM dissociation from CaMKIIδ_C-GFP with excess unlabeled CaM or by lowering $[Ca]_{free}$ is essential. Fig. 1C shows substantial quench of CaMKIIδ_C-GFP WT with the addition of 100 nM F-CaM and its dequench with further addition of 5 μM unlabeled CaM. These patterns indicate that this approach is suitable for measuring changes in CaMKIIδ affinity for CaM.

In permeabilized myocytes, the maximum practical $[Ca]_{free}$ at steady state is ~600 nM, which already causes partial myofilament and tonic myocyte contracture. Any higher $[Ca]_{free}$ causes massive hypercontracture and complete structural collapse of the myocyte, even in the presence of 20 nM cytochalasin D. To maintain cellular structure while elevating $[Ca]_{free}$ to 10–20 μM, and thus approach CaMKII saturation with F-CaM, we removed ATP from the internal solutions. This induces a slight contraction but stable rigor crossbridge formation and myocyte shape. Notably, while global $[Ca]_{free}$ in intact myocytes likely never reaches 10–20 μM, in the cleft between the L-type Ca channel and RyR, the $[Ca]_{free}$ likely exceeds 50 μM during excitation-contraction coupling [43,44]. Since CaMKII and CaM are concentrated at that location [22,27], these are physiologically relevant $[Ca]_{free}$ levels. This approach also allowed us to control whether CaMKIIδ is auto-phosphorylated at Thr 287 in the absence of ATP, by using two well-established mutations that either prevent autophosphorylation (CaMKIIδ_C-GFP T287A) or mimic autophosphorylation (CaMKIIδ_C-GFP T287D) [12,45].

Fig. 2A shows the kinetics of change in both quench of GFP fluorescence intensity (F_{DD}) and FRET ratio signal to F-CaM (F_{DA}) for CaMKIIδ_C -GFP T287A with the addition of 100 nM F-CaM at 20 μM $[Ca]_{free}$ and subsequent addition of 5 μM unlabeled CaM. The mean traces of 3 cells show that the addition of F-CaM reduces donor fluorescence intensity to 60% of its initial value while F_{DA} signal (FRET) increases by 7-fold. To assess the rate of dissociation of F-CaM at 20 μM $[Ca]_{free}$, we added a 50-fold excess of unlabeled CaM (5 μM) so that as F-CaM dissociates, it will be replaced by CaM. This caused F_{DD} dequenching to 80% of its initial intensity and simultaneous decrease in FRET signal (F_{DA}) to half of its peak value. The temporal and inverse relationship of these traces—particularly the donor dequench—are hallmarks of FRET. The incomplete recovery of CaMKIIδ_C-GFP fluorescence intensity is primarily due to incomplete F-CaM dissociation at the high 20 μM $[Ca]_{free}$ over the time course studied, and to a much lesser extent, donor photobleach and diffusion out of the cell.

For this and subsequent experiments, the $[Ca]_{free}$ was increased to 20 μM (from 1 μM in Fig. 1). This is meant to mimic systolic $[Ca]_{free}$ in the dyadic cleft [43], although that level is only transiently attained during systolic SR Ca release. However, it allows us to assess rates of CaM dissociation from a relatively high level of CaMKII saturation. As shown at long times in Fig. 2B, the level of saturation is comparable for the phosphoresistant (T287A) and phosphomimetic (T287D) CaMKIIδ_C.

Fig. 2B compares the rates of F-CaM association (100 nM) to CaMKIIδ_C-GFP T287A vs T287D in saponin-permeabilized cardiac ventricular myocytes. The faster rate of CaM binding to the phosphomimetic CaMKIIδ might suggest that autophosphorylation enhances CaM access to CaMKIIδ_C in myocytes (see Fig. 2D). In this association experiment, the apparent differences between the CaMKIIδ_C-GFP T287A and T287D rates are underestimated due to high $[Ca]_{free}$ (20 μM) and the time required for F-CaM diffusion into the saponin-permeabilized myocytes.

Fig. 2C compares the rates of F-CaM dissociation (100 nM) from CaMKIIδ_C-GFP T287A vs. T287D after adding 5 μM unlabeled CaM in permeabilized ventricular myocytes. F-CaM

readily dissociates from the phosphoresistant T287A mutant, leading to substantial dequench (note inversion of ordinate F_{DD} scale). Conversely, minimal dequench is observed from the phosphomimetic T287D mutant due to slow off-rate of F-CaM and replacement by unlabeled CaM, implying a higher CaM affinity. The initial rates of dissociation during the first 1.5 min for phosphoresistant T287A and first 4 min for phosphomimetic T287D suggest an 11-fold faster CaM dissociation from T287A vs. T287D at $[Ca]_{free}$ of 20 μM.

Fig. 3A shows both phosphoresistant CaMKIIδ_C-GFP T287A fluorescence intensity (F_{DD}) and lifetime (FLT, in ns) in rabbit ventricular myocytes, in the absence (top) or presence of 500 nM F-CaM at 20 μM $[Ca]_{free}$ (bottom). Here, the color-map of FLTs shows relatively spatial-uniform values in the absence of F-CaM (~2.53 ns) and also uniformity with F-CaM (~2.30 ns). The FLTs for the phosphoresistant T287A mutant are dramatically shorter with the addition of 500 nM F-CaM (lower image), which indicates F-CaM binding to CaMKIIδ_C-GFP. FLT in Fig. 3B shows no significant GFP quench by 20 μM $[Ca]_{free}$ without F-CaM or when F-CaM is added (100 nM) at zero $[Ca]_{free}$. These constitute negative controls because CaM is not expected to bind to CaMKIIδ_C under zero $[Ca]_{free}$ conditions. This contrasts to the consistent quench and reduced FLT when both 20 μM $[Ca]_{free}$ and 100 nM F-CaM are present to an average of 2.398 ns (2.379–2.417 ns, 95% CI). Further elevation of [F-CaM] to 500 nM further shortened FLT of phosphoresistant CaMKIIδ_C-GFP T287A to 2.320 ns (2.289–2.351 ns, 95% CI), suggesting increased FRET, CaM-CaMKII binding and possibly altered relative conformation at 500 nM $[Ca]_{free}$.

This FLIM-detected FRET approach allows for discrete comparisons of F-CaM binding to CaMKIIδ_C-GFP T287A vs. T287D under various $[Ca]_{free}$ and F-CaM conditions. Fig. 3C compares the $[Ca]_{free}$-dependence of F-CaM (100 nM) binding to CaMKIIδ_C-GFP T287A vs. T287D. At 0.3 to 1 μM $[Ca]_{free}$ there is much higher F-CaM binding to phosphomimetic T287D vs. T287A. This suggests a very different Ca-dependence of CaM binding to the autophosphorylated CaMKIIδ. Moreover, this indicates substantial CaM binding, especially to autophosphorylated CaMKIIδ over a wide physiological range of global $[Ca]_{free}$ during the Ca cycle in cardiomyocytes (100–600 nM).

Fig. 3D shows steady state saturation binding curves of F-CaM binding to CaMKIIδ_C-GFP T287A and T287D at a fixed 20 μM $[Ca]_{free}$, where CaM should be nearly completely saturated with Ca (as Ca_4CaM). Remarkably, at each [F-CaM], the change in FLT was identical for CaMKIIδ_C-GFP T287A and T287D (K_d = 55.2 nM, h = 1.04 and K_d = 51.7 nM, h = 1.04, respectively). This suggests that under steady-state conditions at high $[Ca]_{free}$, the apparent affinity for Ca_4CaM is similar between autophosphorylated and unphosphorylated CaMKIIδ_C. Importantly, this indicates equivalent starting points for F-CaM binding to CaMKIIδ_C-GFP T287A and T287D for the measurements of dissociation kinetics described below.

The striking differences in $[Ca]_{free}$-dependence of F-CaM binding to CaMKIIδ_C-GFP T287A and T287D (Fig. 3C) despite unaltered Ca_4CaM affinity for T287A vs. T287D (Fig. 3D), has important implications. These results suggest that the phosphomimetic T287D, but not phosphoresistant T287A CaMKII, can uniquely bind partially calcified CaM (Ca_2CaM). Of note, the $[Ca]_{free}$ where the enhanced binding to CaM occurs is closer to the Ca-affinity

of the CaM C-lobe ($K_d \approx 1$ μM) vs. the lower affinity N-lobe sites ($K_d \approx 10$ μM). This is expected to substantially impact the dynamic activation levels of CaMKII during regularly occurring myocyte Ca transients [46].

Our initial attempts to measure F-CaM dissociation in myocytes, shown in Supplementary Figs. S3 and S4, detected much slower F-CaM dissociation from phosphomimetic T287D than phosphoresistant T287A when $[Ca]_{free}$ is reduced from 20 μM to ~20 nM. However, the dissociation time constants (**τ**), in the tens of seconds, were undoubtedly limited by slow changes in myocyte $[Ca]_{free}$ due to flow geometries. A faster and more consistent change in $[Ca]_{free}$ was required for more relevant dissociation measurements.

To more directly assess the kinetics of CaM dissociation as $[Ca]_{free}$ declines during a Ca transient, we established a faster local solution switch very close to the myocyte under observation (see Methods; Supplementary Fig. S5. Fig. 4A shows the kinetics of $[Ca]_{free}$ decline with this system in control myocytes loaded with Fluo-4. The mean **τ** of $[Ca]_{free}$ decline in the bath was 44.5 ± 5.7 ms, which caused a $[Ca]_{free}$ decline in the saponin-permeabilized myocytes with a **τ** = 104.3 ±26 ms (Figs. 4A, Supplementary Fig. S5). These can be visualized in the insets of Fig. 4A, where the bath is essentially black at 110 ms, while the cellular signal that is still visible at this time point disappears over the next 150 ms. This $[Ca]_{free}$ decay is comparable to, but slightly faster than the $[Ca]_{free}$ decline in intact ventricular myocytes (rabbit: **τ** ≈ 290 ms; rat: **τ** ≈ 180 ms) [47]. Thus, F-CaM dissociation from CaMKIIδ$_C$-GFP T287A and T287D can be measured via FRET in myocytes mimicking physiologically relevant $[Ca]_{free}$ decay kinetics.

Fig. 4B shows representative traces of F-CaM dissociation from CaMKIIδ$_C$-GFP T287A and T287D upon rapid Ca chelation. The dequench of CaMKIIδ$_C$-GFP is fit with single-exponential decays to determine the **τ** values of F-CaM dissociation, shown in Fig. 4C. Although the mean **τ** and variance were slightly longer (slower) for CaMKIIδ$_C$-GFP WT (780 ms, 628–933 ms, 95% CI), this was not significantly different from the **τ** of phosphoresistant T287A (569 ms, 462–676 ms, 95% CI; $P = 0.193$). For the phosphomimetic T287D, F-CaM dissociation was nearly 3-fold slower (1399 ms, 1253 ms–1544 ms, 95% CI) than for T287A. This slowed CaM dissociation provides a mechanism for persistent activity seen with autophosphorylated CaMKIIδ in the heart and its significant downstream consequences. The apparently larger variance of **τ** for WT vs. T287A (especially those at long **τ** values) might reflect some CaMKIIδ$_C$ WT being captured in the autophosphorylated state (and overlapping with phosphomimetic T287D **τ** values).

In addition to autophosphorylation at T287, CaMKIIδ can be post-translationally modified by methionine oxidation at 280 and 281 [9]. Fig. 5A shows that individually, high $[Ca]_{free}$, 100 nM F-CaM and 100 μM H_2O_2 had no effect on FLT in T287A CaMKIIδ$_C$-GFP (left 3 sets). However, with 20 μM $[Ca]_{free}$ and 100 nM F-CaM, H_2O_2 induced a significant further reduction in FLT (increased FRET; increased CaM binding), reaching a level equivalent to that achieved with 500 nM F-CaM (20 μM $[Ca]_{free}$, 0 μM H_2O_2). These FLIM-detected FRET measurements suggest that oxidation leads to a combination of increased F-CaM binding to CaMKIIδ$_C$-GFP T287A and possible altered conformation of the CaM-CaMKII

complex (affecting the donor-acceptor distance relationships). Moreover, these oxidative effects on CaM binding occur in the absence of CaMKIIδ autophosphorylation.

Fig. 5B shows the peroxide-free data (from Fig. 4C) as open symbols, alongside parallel F-CaM dissociation kinetic experiments after exposure to 100 μM H_2O_2 (10 min) upon rapid lowering of $[Ca]_{free}$ as in Fig. 4. H_2O_2 exposure did not significantly alter F-CaM dissociation kinetics for either WT or phosphoresistant T287A CaMKIIδ$_C$-GFP, but significantly further delayed F-CaM dissociation from phosphomimetic T287D (1759 ms, 1514–2005 ms, 95% CI). This additional slowing of dissociation from the phosphomimetic T287D suggests potentially synergistic effects of these two PTMs on the duration of CaMKII activation during phasic Ca transients.

4. Discussion

CaMKIIδ is a central mediator of several physiological processes in the heart, and its over-activation is implicated in several diseases [1–6]. Detailing the molecular mechanisms of this increased activity is essential for improving our understanding of CaMKIIδ regulation. Because CaM is the primary activator of CaMKII, understanding how PTMs modulate CaMKIIδ affinity for CaM in cardiac myocytes is of fundamental importance.

To our knowledge, FRET from CaMKIIδ$_C$-GFP and F-CaM is the first reporter for binding between these two proteins in live cardiac myocytes. Figs. 1 and 3 show that this pair yields robust FRET under various experimental conditions with both fluorescence intensity and fluorescence lifetime approaches. The proteins behave as expected physiologically and allow for experiments with F-CaM concentrations similar to endogenous free [CaM] (50–100 nM) in cardiac myocytes [22]. CaMKIIδ$_C$-GFP and F-CaM both localize to the *Z*-lines in the myocyte, as do endogenous CaMKIIδ and CaM, but only directly associate as $[Ca]_{free}$ approaches the micromolar level (Fig. 1) [22,27]. Our estimates of Ca-CaM affinity of CaMKIIδ in cardiac myocytes (K_d ~40 nM; Fig. 3D) are similar to previous in vitro measurements revealing CaMKIIδ as a relatively low affinity target for Ca-CaM (K_d 33.5 ± 13.2) [19]. To load F-CaM onto CaMKIIδ in myocytes with control of both $[Ca]_{free}$ and [F-CaM] required saponin-permeabilization in the physiological myocyte environment. Thus, this system allows quantification of changes in CaMKIIδ affinity for and binding of CaM in cardiac myocytes.

To determine whether autophosphorylation of CaMKIIδ increases its affinity for CaM in cardiac myocytes, we measured rates of F-CaM association to and dissociation from CaMKIIδ$_C$-GFP. Fig. 2 shows faster F-CaM association to phosphomimetic CaMKIIδ$_C$-GFP T287D vs. T287A and much slower dissociation in the presence of excess unlabeled CaM. To our knowledge, these results are the first to confirm that autophosphorylation of CaMKIIδ increases its affinity for CaM in the physiological cardiac myocyte environment. This provides evidence that this mechanism may contribute to persistent CaMKIIδ activity in the heart and its consequent diseases.

Given the Ca dynamics in a beating myocyte, establishing the quantitative relationship between $[Ca]_{free}$ and increased CaMKIIδ affinity for CaM is essential. Fig. 3 demonstrates

that the $[Ca]_{free}$-dependence of CaM-CaMKII association is dramatically shifted in phosphomimetic CaMKIIδ_C T287D, creating significant mechanistic and physiological implications. Interestingly, at 20 μM $[Ca]_{free}$ (sufficient to saturate CaM) and equilibrium conditions, CaMKIIδ_C-GFP T287D and T287A bind identical amounts of F-CaM over the 0 to 500 nM range (Fig. 3C). Importantly, this demonstrates that the two mutants have equivalent starting points for F-CaM dissociation experiments. However, at lower $[Ca]_{free}$, phosphomimetic CaMKIIδ_C-GFP T287D binds F-CaM (100 nM) much more readily than phosphoresistant T287A. That is, at 0.3–1 μM $[Ca]_{free}$, F-CaM binding to CaMKIIδ_C-GFP T287D is nearly saturated whereas binding to CaMKIIδ_C-GFP T287A is less than 30% of its maximal value. This may be explained by an increase in affinity for Ca_2-CaM (CaM bound to 2 Ca ions, likely at the higher affinity C-lobe sites) upon autophosphorylation [28,48]. Physiologically, this greatly increases the range of $[Ca]_{free}$ in which CaM will remain bound to—and promote—autophosphorylated CaMKIIδ activity.

This $[Ca]_{free}$-dependence of phosphomimetic CaMKIIδ_C T287D implies that CaMKIIδ_C which is autophosphorylated in the junctional cleft region at the *Z*-line (where CaMKII ought to be preferentially activated by the very high, >50 μM $[Ca]_{free}$ achieved) [14] may remain relatively activated. Notably, such activation also promotes CaMKIIδ mobility as it translocates from the Z-line to other myocyte loci under conditions where CaMKIIδ is activated or phosphomimetic (T287D) [27]. That is, even at bulk cytosolic $[Ca]_{free}$ in the 200–400 nM range could sustain CaMKIIδ activation and enable it to phosphorylate cytosolic proteins like phospholamban and histone deacetylases, which reside in micro-environments where local $[Ca]_{free}$ would almost never be sufficiently high to directly activate non-autophosphorylated CaMKIIδ [14].

To further test the relevance of this $[Ca]_{free}$-dependent increase in CaM binding to autophosphorylated CaMKIIδ in the heart, we also quantified the kinetics of CaM dissociation during physiological $[Ca]_i$ decline. To do this, we created a system to rapidly lower $[Ca]_{free}$ in permeabilized myocytes with similar kinetics as occurs during normal heartbeats in intact myocytes (Fig. 4A) [47]. Fig. 4C shows that autophosphorylation causes a 3-fold slowing of F-CaM dissociation from CaMKIIδ. With a time-constant >1 s, this greatly increases the likelihood that CaM remains bound—and CaMKIIδ remains active—through one Ca transient and into the next. This is consistent with a frequency-dependent CaMKII activation in adult rabbit myocytes, as we have previously reported [18] over the 0 to 1 Hz range, with autophosphorylation being recruited especially above 1 Hz frequencies.

Autophosphorylation requires CaM binding to both the phosphorylating subunit and the neighboring target subunit in the dodecameric holoenzyme structure [49]. Indeed, the very high $[Ca]_{free}$ levels achieved in the junctional cleft (or prolongation thereof) would promote coincidental Ca_4CaM binding at these adjacent CaMKII monomers, thereby facilitating autophosphorylation of CaMKIIδ [14,50]. At the cellular level, changes in Ca handling and effects on other targets induced by increased CaMKIIδ activity can lead to feedforward loops that further enhance autophosphorylation and potentially promote other PTMs [1,5,28,51].

Oxidation, *O*-GlcNAcylation and *S*-nitrosylation can, like autophosphorylation, also lead to persistent CaMKIIδ activity [9–11]. It was previously unknown whether CaMKIIδ oxidation leads to persistent activity by increasing its affinity for CaM or whether it synergizes with autophosphorylation. Fig. 5A shows that oxidation increases F-CaM association to CaMKIIδ_C-GFP T287A. In the presence of 100 μM H_2O_2, 100 nM F-CaM generates a FLT change comparable to much higher (500 nM) F-CaM without H_2O_2. Because these experiments were conducted at high $[Ca]_{free}$ (20 μM), part of this effect could be due to higher saturation by F-CaM (e.g. Fig. 3D), but we cannot rule out the possibility that CaMKII oxidation alters the CaM-CaMKII conformation and/or average distance between the fluorophores. In this regard, potential oxidation of CaM itself is limited by our use of F-CaM that has no free cysteines [34,52].

Interestingly, Fig. 5B shows that these oxidative effects do not translate to slower F-CaM dissociation from CaMKIIδ_C-GFP WT or T287A upon rapid lowering of $[Ca]_{free}$. However, H_2O_2 further slowed F-CaM dissociation from CaMKIIδ_C-GFP T287D. This corroborates an additive effect of autophosphorylation and oxidation observed in our previous study, in terms of both an increase in CaMKIIδ activity as well as a persistence in an open autonomous conformational state [18]. Based on those activating effects of oxidation and the reduced FLIM by oxidation in T287A in Fig. 5A, we had expected a concomitant slowing in F-CaM dissociation kinetics in response to oxidation in CaMKIIδ_C-GFP WT or T287A, but this was not the case. Oxidation of WT or T287A CaMKIIδ had no effect on F-CaM off rate, but it further slowed F-CaM dissociation from phosphomimetic T287D CaMKIIδ. We conclude that oxidation of CaMKIIδ can promote the open autonomous state [18] and that conformational effect may be why fluorescence lifetime was reduced in Fig. 5A, but by itself that did not slow CaM off-rate from this presumed autonomous open state. These interactions add to the complexity of CaMKIIδ regulation and implicate PTM-induced changes in CaM affinity in additional feedback loops and disease regimes.

This work validates a novel FRET reporter for CaM binding to CaMKIIδ in live cardiac myocytes. We showed that autophosphorylation of CaMKIIδ increases affinity for CaM in its native environment and that this increase is dependent on $[Ca]_{free}$. This leads to much slower CaM dissociation from CaMKIIδ when $[Ca]_{free}$ is rapidly reduced. Furthermore, the interaction of autophosphorylation and oxidation leads to even slower CaM dissociation. Together, these data create a compelling case for increased CaM affinity as a mechanism of persistent CaMKIIδ activity in the heart and its associated diseases.

This experimental system creates a framework for quantifying the effects of other PTMs (ROS, *S*-nitrosylation, *O*-GlcNAcylation) on CaMKIIδ affinity for CaM and their interactions. We demonstrated that autophosphorylation slows CaM dissociation from CaMKIIδ, but we have yet to quantify changes in association rates with physiologically relevant kinetics. Logically, CaM association with CaMKIIδ at lower $[Ca]_{free}$ seen globally in the cytosol further increases the spatiotemporal window of CaM binding to CaMKIIδ and target phosphorylation. Our well-controlled studies here create quantitative constraints for the interpretation of future studies in intact electrically paced myocytes, which are inherently less controlled with respect to $[Ca]_{free}$ and [CaM]. Nevertheless, those will be required to more fully test the real in situ dynamics of CaM-CaMKIIδ interaction and to further

update computational models [14,51]. Furthermore, using CaM mutants to probe whether autophosphorylation increases CaMKIIδ affinity for Ca_2-CaM would be informative.

Supplementary Material

Refer to Web version on PubMed Central for supplementary material.

Acknowledgements

We thank Julie Bossuyt, Benjamin W. Van, Maura Ferrero, Bence Hegyi, and Kenneth S. Ginsburg for their help in animal care, cell isolation, and technical support and advice.

Funding

This work was supported by an American Heart Association fellowship 19PRE34450010 (MS) and NIH grants P01-HL141084 (DMB), R01-HL142282 (DMB), R01-HL092097 (DMB and RLC), R01-HL1385391 (DMB and RLC), R37-AG026160 (RLC), F32-HL144017 (CYK).

References

[1]. Anderson ME, Brown JH, Bers DM, CaMKII in myocardial hypertrophy and heart failure, J. Mol. Cell. Cardiol. 51 (4) (2011) 468–473. [PubMed: 21276796]

[2]. Bers DM, Grandi E, Calcium/calmodulin-dependent kinase II regulation of cardiac ion channels, J. Cardiovasc. Pharmacol. 54 (3) (2009) 180–187. [PubMed: 19333131]

[3]. Bers DM, Ca^{2+}-calmodulin-dependent protein kinase II regulation of cardiac excitation-transcription coupling, Heart Rhythm. 8 (7) (2011) 1101–1104. [PubMed: 21255680]

[4]. Maier LS, Role of CaMKII for signaling and regulation in the heart, Front. Biosci. (Landmark Ed.) 14 (2009) 486–496. [PubMed: 19273080]

[5]. Hegyi B, Bers DM, Bossuyt J, CaMKII signaling in heart diseases: emerging role in diabetic cardiomyopathy, J. Mol. Cell. Cardiol. 127 (2019) 246–259. [PubMed: 30633874]

[6]. Dewenter M, von der Lieth A, Katus HA, Backs J, Calcium signaling and transcriptional regulation in cardiomyocytes, Circ. Res. 121 (8) (2017) 1000–1020. [PubMed: 28963192]

[7]. Zhang T, Maier LS, Dalton ND, Miyamoto S, Ross J Jr., D.M. Bers, J.H. Brown, The deltaC isoform of CaMKII is activated in cardiac hypertrophy and induces dilated cardiomyopathy and heart failure, Circ. Res. 92 (8) (2003) 912–919. [PubMed: 12676814]

[8]. Westenbrink BD, Edwards AG, McCulloch AD, Brown JH, The promise of CaMKII inhibition for heart disease: preventing heart failure and arrhythmias, Expert Opin. Ther. Targets 17 (8) (2013) 889–903. [PubMed: 23789646]

[9]. Erickson JR, Joiner ML, Guan X, Kutschke W, Yang J, Oddis CV, Bartlett RK, Lowe JS, O'Donnell SE, Aykin-Burns N, Zimmerman MC, Zimmerman K, Ham AJ, Weiss RM, Spitz DR, Shea MA, Colbran RJ, Mohler PJ, Anderson ME, A dynamic pathway for calcium-independent activation of CaMKII by methionine oxidation, Cell 133 (3) (2008) 462–474. [PubMed: 18455987]

[10]. Erickson JR, Nichols CB, Uchinoumi H, Stein ML, Bossuyt J, Bers DM, S-nitrosylation induces both autonomous activation and inhibition of calcium/ calmodulin-dependent protein kinase II δ, J. Biol. Chem. 290 (42) (2015) 25646–25656. [PubMed: 26316536]

[11]. Erickson JR, Pereira L, Wang L, Han G, Ferguson A, Dao K, Copeland RJ, Despa F, Hart GW, Ripplinger CM, Bers DM, Diabetic hyperglycaemia activates CaMKII and arrhythmias by O-linked glycosylation, Nature 502 (7471) (2013) 372–376. [PubMed: 24077098]

[12]. Meyer T, Hanson PI, Stryer L, Schulman H, Calmodulin trapping by calcium-calmodulin-dependent protein kinase, Science 256 (5060) (1992) 1199–1202. [PubMed: 1317063]

[13]. Edman CF, Schulman H, Identification and characterization of delta B-CaM kinase and delta C-CaM kinase from rat heart, two new multifunctional Ca^{2+}/ calmodulin-dependent protein kinase isoforms, Biochim. Biophys. Acta 1221 (1) (1994) 89–101. [PubMed: 8130281]

[14]. Saucerman JJ, Bers DM, Calmodulin mediates differential sensitivity of CaMKII and calcineurin to local Ca^{2+} in cardiac myocytes, Biophys. J. 95 (10) (2008) 4597–4612. [PubMed: 18689454]

[15]. Miller SG, Kennedy MB, Regulation of brain type II Ca^{2+}/calmodulin-dependent protein kinase by autophosphorylation: a Ca^{2+}-triggered molecular switch, Cell 44 (6) (1986) 861–870. [PubMed: 3006921]

[16]. Bradshaw JM, Hudmon A, Schulman H, Chemical quenched flow kinetic studies indicate an intraholoenzyme autophosphorylation mechanism for Ca^{2+}/ calmodulin-dependent protein kinase II, J. Biol. Chem. 277 (23) (2002) 20991–20998. [PubMed: 11925447]

[17]. Coultrap SJ, Buard I, Kulbe JR, Dell'Acqua ML, Bayer KU, CaMKII autonomy is substrate-dependent and further stimulated by Ca^{2+}/calmodulin, J. Biol. Chem. 285 (23) (2010) 17930–17937. [PubMed: 20353941]

[18]. Erickson JR, Patel R, Ferguson A, Bossuyt J, Bers DM, Fluorescence resonance energy transfer-based sensor Camui provides new insight into mechanisms of calcium/calmodulin-dependent protein kinase II activation in intact cardiomyocytes, Circ. Res. 109 (7) (2011) 729–738. [PubMed: 21835909]

[19]. Gaertner TR, Kolodziej SJ, Wang D, Kobayashi R, Koomen JM, Stoops JK, Waxham MN, Comparative analyses of the three-dimensional structures and enzymatic properties of alpha, beta, gamma and delta isoforms of Ca^{2+}-calmodulin-dependent protein kinase II, J. Biol. Chem. 279 (13) (2004) 12484–12494. [PubMed: 14722083]

[20]. Lu S, Liao Z, Lu X, Katschinski DM, Mercola M, Chen J, Heller Brown J, Molkentin JD, Bossuyt J, Bers DM, Hyperglycemia acutely increases cytosolic reactive oxygen species via O-linked GlcNAcylation and CaMKII activation in mouse ventricular myocytes, Circ. Res. 126 (10) (2020) e80–e96. [PubMed: 32134364]

[21]. Bayer KU, De Koninck P, Leonard AS, Hell JW, Schulman H, Interaction with the NMDA receptor locks CaMKII in an active conformation, Nature 411 (6839) (2001) 801–805. [PubMed: 11459059]

[22]. Wu X, Bers DM, Free and bound intracellular calmodulin measurements in cardiac myocytes, Cell Calcium 41 (4) (2007) 353–364. [PubMed: 16999996]

[23]. Hudmon A, Schulman H, Kim J, Maltez JM, Tsien RW, Pitt GS, CaMKII tethers to L-type Ca^{2+} channels, establishing a local and dedicated integrator of Ca^{2+} signals for facilitation, J. Cell Biol. 171 (3) (2005) 537–547. [PubMed: 16275756]

[24]. Ai X, Curran JW, Shannon TR, Bers DM, Pogwizd SM, Ca^{2+}/calmodulin- dependent protein kinase modulates cardiac ryanodine receptor phosphorylation and sarcoplasmic reticulum Ca^{2+} leak in heart failure, Circ. Res. 97 (12) (2005) 1314–1322. [PubMed: 16269653]

[25]. Singh P, Salih M, Tuana BS, Alpha-kinase anchoring protein alphaKAP interacts with SERCA2A to spatially position Ca^{2+}/calmodulin-dependent protein kinase II and modulate phospholamban phosphorylation, J. Biol. Chem. 284 (41) (2009) 28212–28221. [PubMed: 19671701]

[26]. Faul C, Dhume A, Schecter AD, Mundel P, Protein kinase A, Ca^{2+}/calmodulin-dependent kinase II, and calcineurin regulate the intracellular trafficking of myopodin between the Z-disc and the nucleus of cardiac myocytes, Mol. Cell. Biol. 27 (23) (2007) 8215–8227. [PubMed: 17923693]

[27]. Wood BM, Simon M, Galice S, Alim CC, Ferrero M, Pinna NN, Bers DM, Bossuyt J, Cardiac CaMKII activation promotes rapid translocation to its extra- dyadic targets, J. Mol. Cell. Cardiol. 125 (2018) 18–28. [PubMed: 30321537]

[28]. Saucerman JJ, Bers DM, Calmodulin binding proteins provide domains of local Ca^{2+} signaling in cardiac myocytes, J. Mol. Cell. Cardiol. 52 (2) (2012) 312–316. [PubMed: 21708171]

[29]. Song Q, Saucerman JJ, Bossuyt J, Bers DM, Differential integration of Ca^{2+}-calmodulin signal in intact ventricular myocytes at low and high affinity Ca^{2+}-calmodulin targets, J. Biol. Chem. 283 (46) (2008) 31531–31540. [PubMed: 18790737]

[30]. Maier LS, Ziolo MT, Bossuyt J, Persechini A, Mestril R, Bers DM, Dynamic changes in free Ca-calmodulin levels in adult cardiac myocytes, J. Mol. Cell. Cardiol. 41 (3) (2006) 451–458. [PubMed: 16765983]

[31]. Bassani RA, Bers DM, Na-Ca exchange is required for rest-decay but not for rest- potentiation of twitches in rabbit and rat ventricular myocytes, J. Mol. Cell. Cardiol. 26 (10) (1994) 1335–1347. [PubMed: 7869394]

[32]. Bartos DC, Morotti S, Ginsburg KS, Grandi E, Bers DM, Quantitative analysis of the Ca^{2+}-dependent regulation of delayed rectifier K^+ current I_{Ks} in rabbit ventricular myocytes, J. Physiol. (London) 595 (7) (2017) 2253–2268. [PubMed: 28008618]

[33]. Bers DM, Patton CW, Nuccitelli R, A practical guide to the preparation of Ca, in a practical guide to the study of calcium in living cells, Meth. Cell Biol. 40 (1994) 93–113.

[34]. Fruen BR, Balog EM, Schafer J, Nitu FR, Thomas DD, Cornea RL, Direct detection of calmodulin tuning by ryanodine receptor channel targets using a Ca^{2+}-sensitive acrylodan-labeled calmodulin, Biochemistry 44 (1) (2005) 278–284. [PubMed: 15628869]

[35]. Rasband WS, ImageJ, National Institutes of Health, Bethseda, Maryland, USA, 1997-2018.

[36]. Oliphant TE, A guide to NumPy, Trelgol Publishing, USA, 2006.

[37]. Virtanen P, Gommers R, Oliphant TE, Haberland M, Reddy T, Cournapeau D, Burovski E, Peterson P, Weckesser W, Bright J, van der Walt SJ, Brett M, Wilson J, Millman KJ, Mayorov N, Nelson ARJ, Jones E, Kern R, Larson E, Carey CJ, Polat I, Feng Y, Moore EW, VanderPlas J, Laxalde D, Perktold J, Cimrman R, Henriksen I, Quintero EA, Harris CR, Archibald AM, Ribeiro AH, Pedregosa F, van Mulbregt P, SciPy 1.0: fundamental algorithms for scientific computing in Python, Nat. Methods 17 (3) (2020) 261–272. [PubMed: 32015543]

[38]. Hunter JD, Matplotlib: a 2D graphics environment, Comput. Sci. Engin. 9 (3) (2007) 90–95.

[39]. Köllner M, Wolfrum J, How many photons are necessary for fluorescence-lifetime measurements? Chem. Phys. Lett. 200 (1–2) (1992) 199–204.

[40]. Becker W, Bergmann A, Biscotti G, Koenig K, Riemann I, Kelbauskas L, Biskup C, High-speed FLIM data acquisition by time-correlated single-photon counting, in: Multiphoton Microscopy in the Biomedical Sciences IV, International Society for Optics and Photonics, 2004, pp. 27–35.

[41]. Yang Y, Guo T, Oda T, Chakraborty A, Chen L, Uchinoumi H, Knowlton AA, Fruen BR, Cornea RL, Meissner G, Cardiac myocyte Z-line calmodulin is mainly RyR2-bound, and reduction is arrhythmogenic and occurs in heart failure, Circ. Res. 114 (2) (2014) 295–306. [PubMed: 24186966]

[42]. Quintana AR, Wang D, Forbes JE, Waxham MN, Kinetics of calmodulin binding to calcineurin, Biochem. Biophys. Res. Comm. 334 (2) (2005) 674–680. [PubMed: 16009337]

[43]. Bers DM, Excitation-Contraction Coupling and Cardiac Contractile Force, Kluwer Academic Press, Dordrecht, Netherlands, 2001, 427 pp.

[44]. Shannon TR, Wang F, Puglisi J, Weber C, Bers DM, A mathematical treatment of integrated Ca dynamics within the ventricular myocyte, Biophys. J. 87 (5) (2004) 3351–3371. [PubMed: 15347581]

[45]. Mayford M, Wang J, Kandel ER, O'Dell TJ, CaMKII regulates the frequency-response function of hippocampal synapses for the production of both LTD and LTP, Cell 81 (6) (1995) 891–904. [PubMed: 7781066]

[46]. De Koninck P, Schulman H, Sensitivity of CaM kinase II to the frequency of Ca^{2+} oscillations, Science 279 (5348) (1998) 227–230. [PubMed: 9422695]

[47]. Bers DM, Berlin JR, Kinetics of $[Ca]_i$ decline in cardiac myocytes depend on peak $[Ca]_i$, Am. J. Phys. 268 (1 Pt 1) (1995) C271–C277.

[48]. Shifman JM, Choi MH, Mihalas S, Mayo SL, Kennedy MB, Ca2+/calmodulin- dependent protein kinase II (CaMKII) is activated by calmodulin with two bound calciums, Proc. Natl. Acad. Sci. U. S. A. 103 (38) (2006) 13968–13973. [PubMed: 16966599]

[49]. Rich RC, Schulman H, Substrate-directed function of calmodulin in autophosphorylation of Ca^{2+}/calmodulin-dependent protein kinase II, J. Biol. Chem. 273 (43) (1998) 28424–28429. [PubMed: 9774470]

[50]. Johnson DE, Meng J, Hudmon A, Mechanisms underlying cooperativity in CaMKII autophosphorylation and substrate phosphorylation, Biophys. J. 106 (2) (2014) 528a.

[51]. Morotti S, Edwards AG, McCulloch AD, Bers DM, Grandi E, A novel computational model of mouse myocyte electrophysiology to assess the synergy between Na^+ loading and CaMKII, J. Physiol. 592 (6) (2014) 1181–1197. [PubMed: 24421356]

[52]. Kortvely E, Gulya K, Calmodulin, and various ways to regulate its activity, Life Sci. 74 (9) (2004) 1065–1070. [PubMed: 14687647]

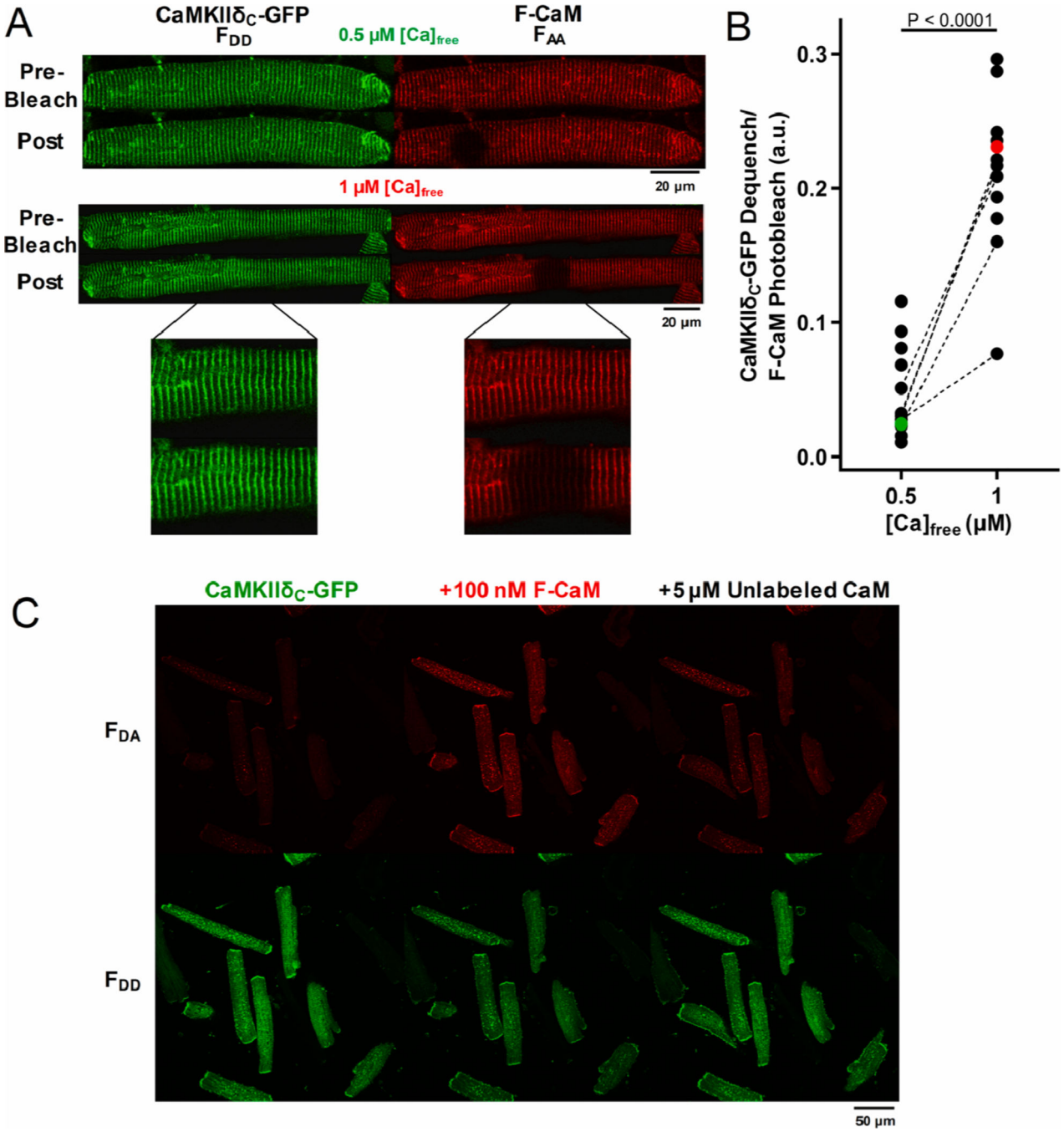

Fig. 1.

Elevated $[Ca]_{free}$ allows FRET as a dynamic reporter of F-CaM binding to CaMKIIδ in cardiac ventricular myocytes for fluorescence intensity approaches.

A) At 0.5 μM $[Ca]_{free}$ (upper cell), CaMKIIδ$_C$-GFP WT dequench is minimal after acceptor F-CaM (100 nM) photobleach in cardiac ventricular myocytes. This cell is denoted by the green symbol in panel B. CaMKIIδ$_C$-GFP WT dequench is greater at 1 μM $[Ca]_{free}$ (upper cell) after acceptor photobleach. This cell is denoted by the red symbol in panel B. F_{DD} is donor (CaMKIIδ$_C$-GFP) fluorescence intensity with donor excitation (488 nm),

and F_{AA} is acceptor F-CaM fluorescence intensity with acceptor excitation (561 nm). B) CaMKIIδ_C-GFP dequench is greater after acceptor (100 nM) F-CaM photobleach at higher $[Ca]_{free}$. n = 7 cells/ condition, plus 5 paired (19 total); unpaired *t*-test; P-values are as indicated in the figure. C) CaMKIIδ_C–GFP WT (F_{DD}) and F-CaM fluorescence intensity with donor excitation (F_{DA}) in cardiac ventricular myocytes before and after addition of 100 nM F-CaM and after addition of 5 μM unlabeled CaM at 1 μM $[Ca]_{free}$.

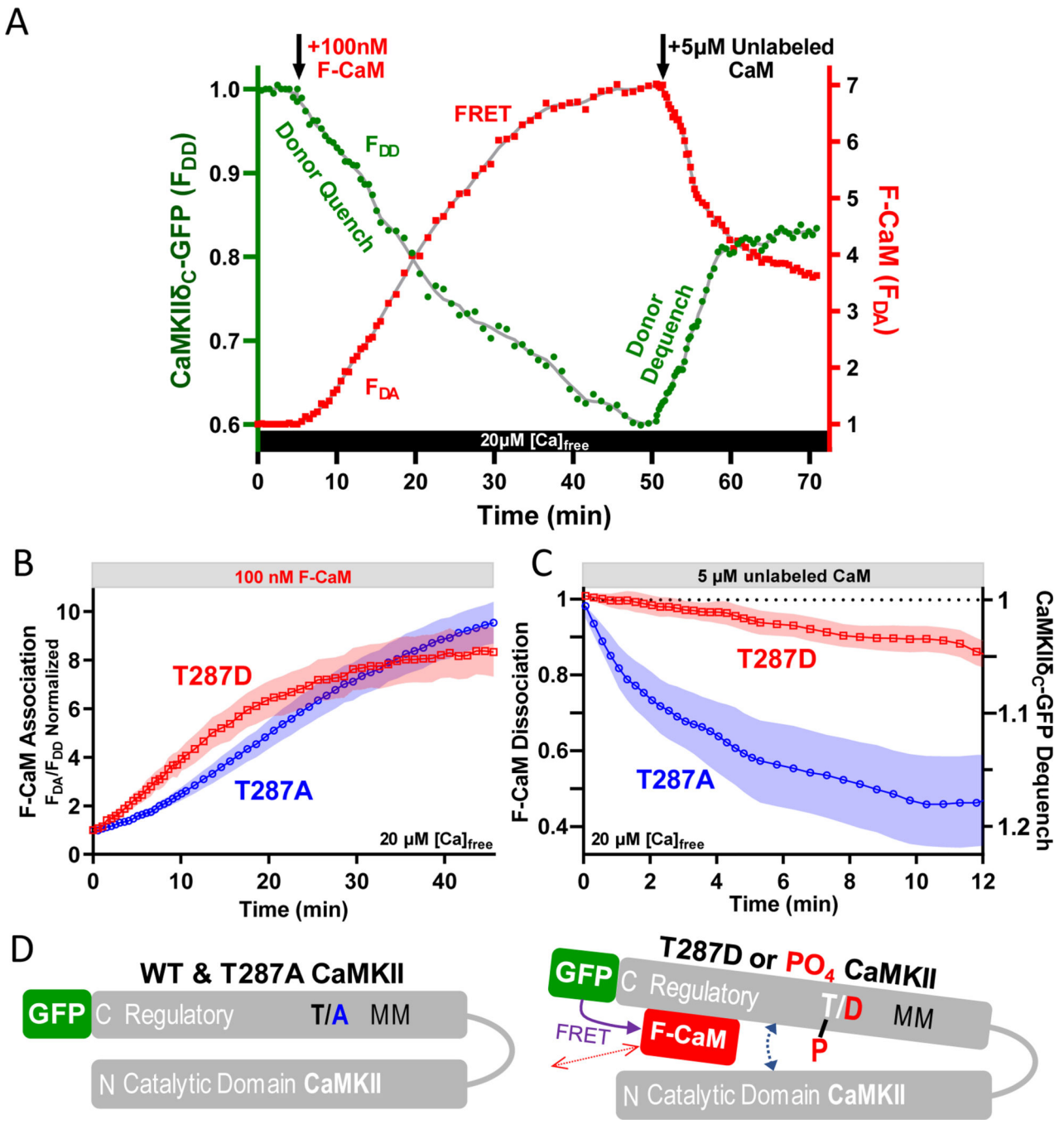

Fig. 2.

Autophosphorylation increases the rate of F-CaM association to CaMKIIδ in cardiac ventricular myocytes and slows its dissociation.

A) Mean timecourse of CaMKIIδ_C–GFP TA (F_{DD}) and F-CaM fluorescence intensity with donor excitation (F_{DA}, FRET) in 3 cardiac ventricular myocytes after the addition of 100 nM F-CaM, and after addition of 5 μM unlabeled CaM at 20 μM $[Ca]_{free}$. B) F-CaM (100 nM) association to CaMKIIδ_C-GFP T287A vs T287D in permeabilized ventricular myocytes at 20 μM $[Ca]_{free}$. Mean traces with 95% CI. N/n (animals/cells): T287A, 3/30; T287D, 3/18.

C) F-CaM (100 nM) dissociation from CaMKIIδ_C-GFP T287A vs T287D after addition of 5 μM unlabeled CaM in permeabilized cardiac myoctes 20 μM $[Ca]_{free}$. Mean traces with 95% CI. N/n (animals/cells) = T287A, 3/19; T287D, 3/15. D).

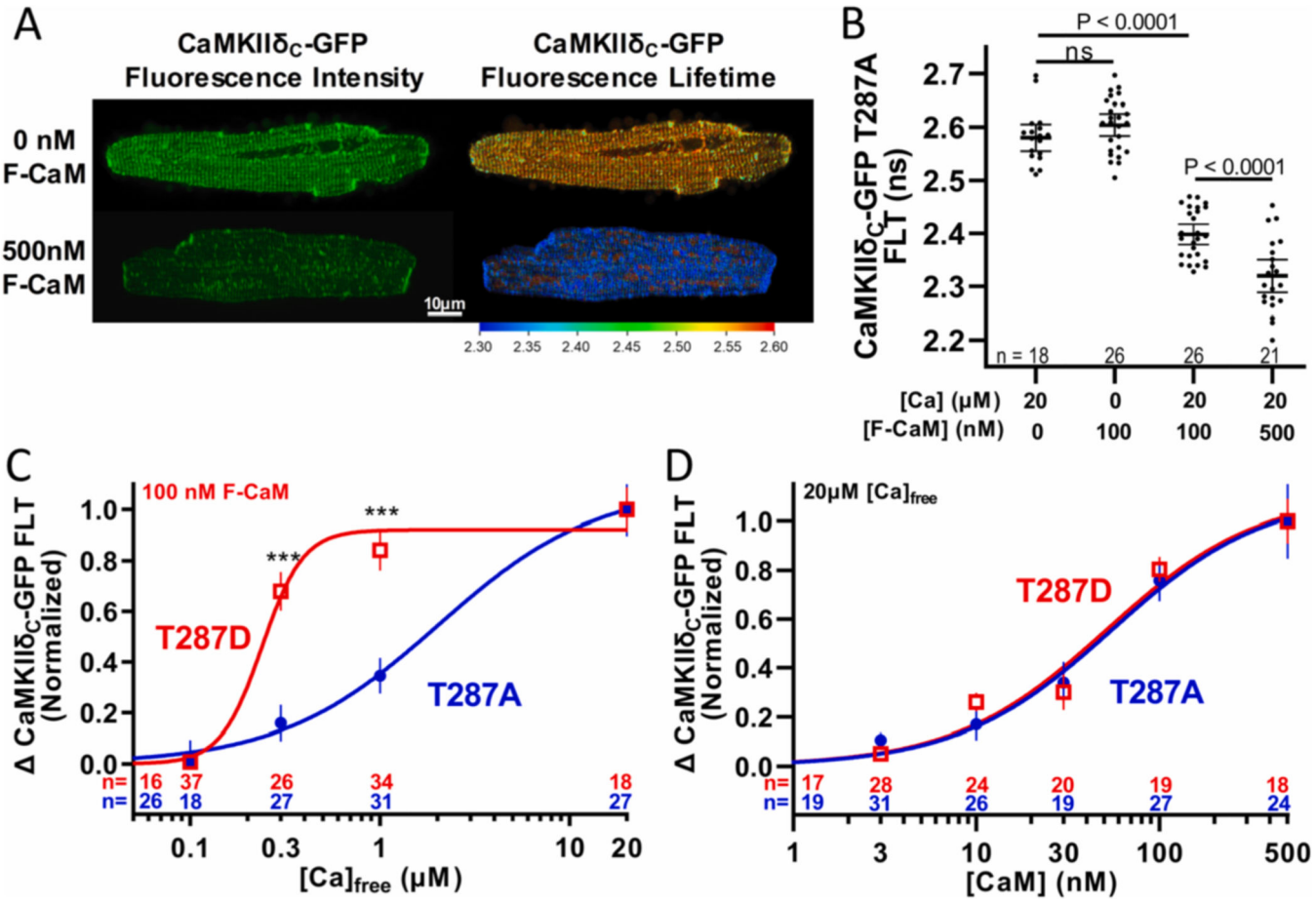

Fig. 3.

Autophosphorylation confers increased F-CaM binding to CaMKIIδ in cardiac ventricular myocytes at lower $[Ca]_{free}$ but not at steady-state high $[Ca]_{free}$ conditions. A) Fluorescence intensity images of permeabilized rabbit ventricular myocytes expressing CaMKIIδ_C-GFP T287A (phosphoresistant) (left) overlaid with mask of fluorescence lifetimes (FLTs) (right). Scale bar below denotes FLTs in ns. The cell in upper images is in 0 nM acceptor F-CaM internal solution yielding unquenched FLTs. Cell in lower images is in 500 nM F-CaM, shortening donor FLTs due to FRET. B) CaMKIIδ_C–GFP T287A FLTs in rabbit ventricular myocytes in internal solutions with Ca_{free} and F-CaM concentrations to determine unquenched and quenched FLTs. n (cells/ condition) are in figure; mean and 95% CI; Tukey's Multiple Comparison; P-values are as indicated in the figure. C) Normalized change in FLT-detected FRET of CaMKIIδ_C-GFP T287A vs T287D (phosphomimetic) in permeabilized ventricular cardiomyocytes monitors F-CaM (100 nM) binding in internal solutions with $[Ca]_{free}$, from <20 nM to 20 μM. n (cells/condition) are indicated in figure; mean with 95% CI. *** P <0.0001 T287A vs T287D at 0.3 and 1 μM $[Ca]_{free}$, Tukey's Multiple Comparison. First n-values are for nominally 0 nM Ca (not readily represented on log scale). D) Normalized change in FLT-detected FRET of CaMKIIδ_C-GFP T287A vs T287D in permeabilized ventricular cardiomyocytes in response to 0–500 nM F-CaM in 20 μM $[Ca]_{free}$ internal solution. n (cells/condition) are indicated in figure; mean with 95% CI; first n-values are for 0 nM CaM.

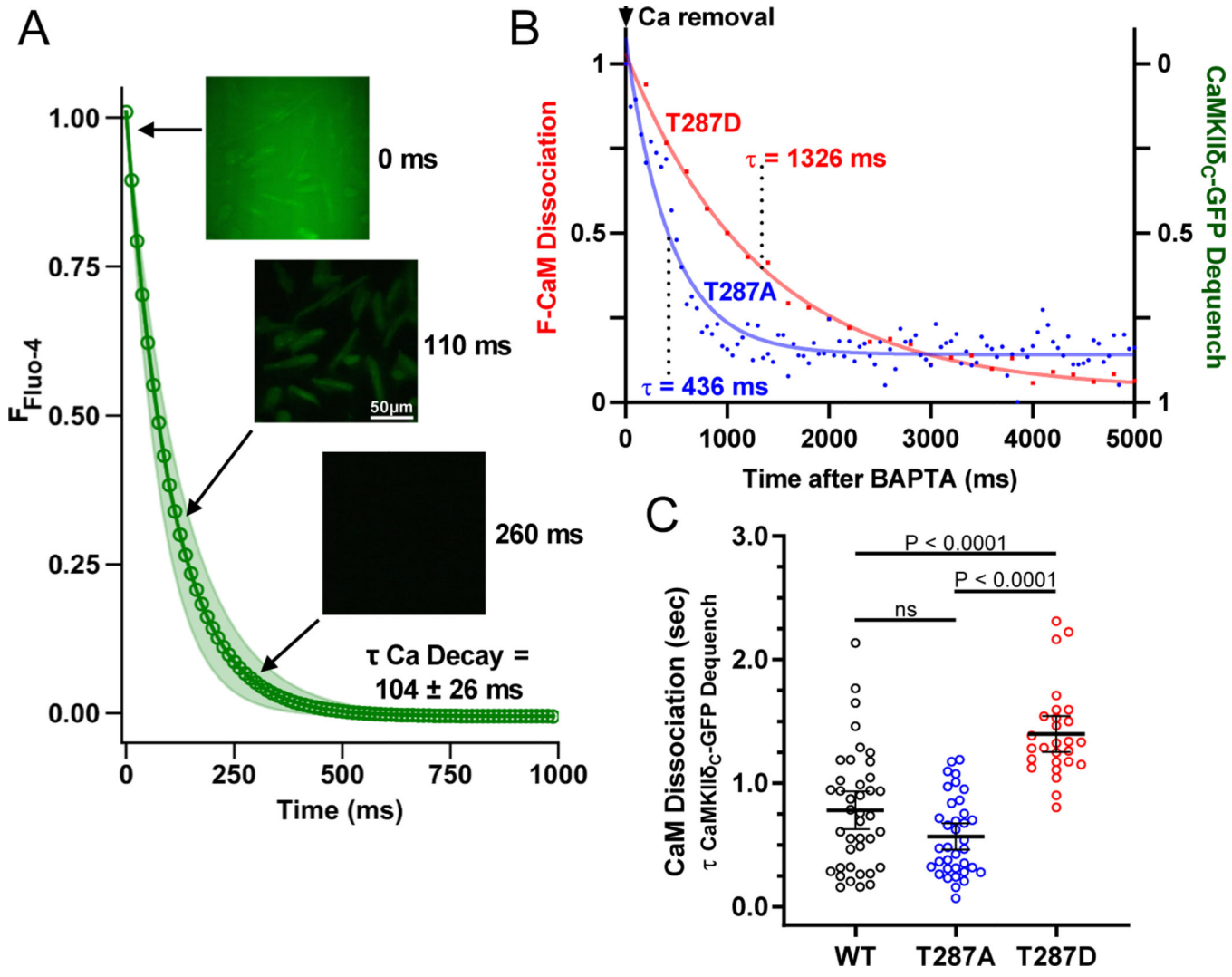

Fig. 4.

Autophosphorylation slows F-CaM dissociation from CaMKIIδ in cardiac ventricular myocytes upon lowering $[Ca]_{free}$ with physiological kinetics. A) Kinetics of Ca chelation in cardiac ventricular myocytes upon local delivery of BAPTA internal solution with representative inset images of wells at indicated timepoints. Myocytes were loaded with 30 μM Fluo-4 salt in 20 μM $[Ca]_{free}$ internal solution. $n = 53$ cells; mean trace with 95% CI. B) Representative time course of CaMKIIδ$_C$-GFP T287A (phosphoresistant) vs. T287D (phosphomimetic) dequench due to dissociation from 100 nM F-CaM after local delivery of BAPTA internal solution. Curves are exponential fits to estimate **τ** of dissociation. C) **τ** of F-CaM (100 nM) dissociation from CaMKIIδ$_C$-GFP WT, T287A, and T287D upon local delivery of BAPTA internal solution. N/n (animals/cells): 5/40 (WT), 4/36 (T287A), and 2/27 (T287D) cells; mean with 95% CI; Dunnett's Multiple Comparison; *P*-values are as indicated in the figure.

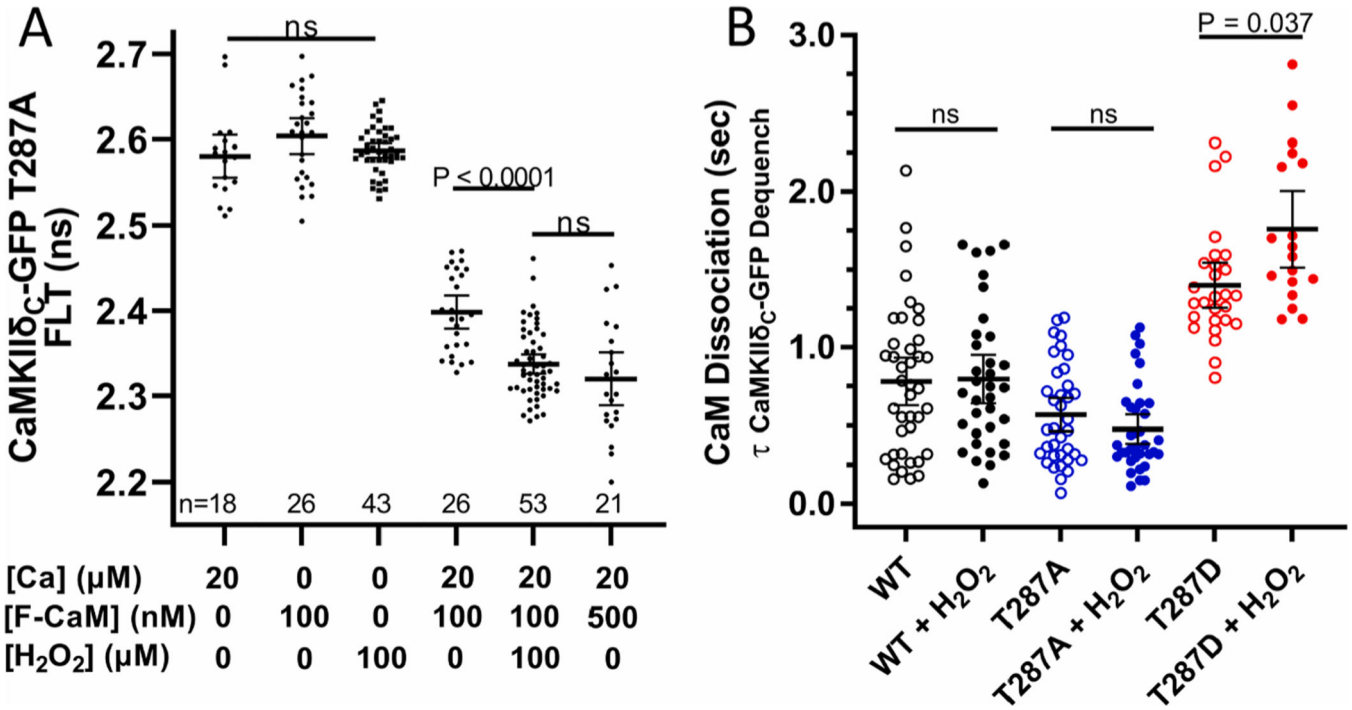

Fig. 5.

Oxidation increases F-CaM association with CaMKIIδ in cardiac ventricular myocytes and with autophosphorylation, further slows F-CaM dissociation upon lowering $[Ca]_{free}$. A) CaMKIIδ_C-GFP T287A (phosphoresistant) FLT measurements in rabbit ventricular myocytes in internal solutions with Ca_{free} and F-CaM concentrations ± 100 μM H_2O_2 to determine oxidation effect on FRET (F-CaM binding). n (cells/condition) are indicated in figure; mean with 95% CI; Dunnett's Multiple Comparison; P-values are indicated in figure. B) τ of F-CaM (100 nM) dissociation from CaMKIIδ_C-GFP WT, T287A (phosphoresistant), and T287D (phosphomimetic) ± 100 μM H_2O_2 upon local delivery of BAPTA internal solution. Data without H_2O_2 same as shown in Fig. 4C. N/n (animals/cells): 5/40 (WT), 3/34 (WT + H_2O_2), 4/36 (T287A), 5/35 (T287A + H_2O_2), 2/27 (T287D), and 3/18 (T287D + H_2O_2) cells; mean with 95% CI; Dunnett's Multiple Comparison; P-values are indicated in figure.